Transactions of the Korean Society of Mechanical Engineers, Vol. 8, No.3, pp. 241～249, 1984.

<**Original**>

Natural Convection from a Horizontal Cylinder with Two Long Vertical Axial Fins

Sun Sok Kwon

(Received December 6, 1983)

두 垂直 平板핀을 가진 水平圓筒으로 부터의 自然對流

權 純 錫

抄 錄

두 개의 긴 垂直平板핀을 가진 等溫水平圓筒으로 부터의 自然對流 熱傳達을 2次元 有限差分法에 의한 數値解析으로 硏究하였다.

軸方向의 두 垂直平板핀을 가진 水平圓筒으로 부터의 熱傳達은 $Ra=10^6$, $Pr=5$ 및 無次元핀 變數 $K_f t/KD=0.5$ 인 경우에 보통 圓筒에서의 熱傳達보다 5.32% 增加되었다. Ra 와 Pr 가 增加하면 局所핀 누셀트數는 增加하고 無次元핀 溫度는 減少된다. 그러나 無次元핀 變數가 增加하면 局所핀 누셀트數와 無次元핀 溫度分布는 增加된다.

最大局所핀 누셀트數는 $Ra=10^6$ 인 경우에 上向핀과 下向핀의 $(r-r_0)=0.1\sim0.2$ 에서 存在한다. 垂直핀을 가진 원통주위에서 浮力 誘導된 流動은 보통 원통에서 보다 더욱 活發하였다. 따라서 $Ra=10^6$, $Pr=5$ 인 경우에 핀 近方에서의 無次元 半徑方向 速度는 보통원통의 경우보다 큰 값을 가진다.

Nomenclature

C_f : Dimensionless fin parameter, $k_f\, t/kD$

D : Cylinder diameter

h : Cylinder local heat transfer coefficient, $q/\Delta T$

h_f : Fin local heat transfer coefficient, $q/\Delta T_f$

g : Gravitational acceleration

k : Thermal conductivity of fluid

k_f : Thermal conductivity of fin

Nu : Local Nusselt number, hD/k

Pr : Prandtl number

Q : Heat transfer rate per unit length of cylinder

q : Local heat transfer rate

R : Radial coordinate

r : Dimensionless radial coordinate, R/D

Ra : Rayleigh number, $g\beta D^3 \Delta T/\nu\alpha$

T : Temperature

T_∞ : Ambient fluid temperature

ΔT : Temperature difference, T_0-T_∞

ΔT_f : Temperature difference, T_f-T_∞

t : Fin half thickness

u : Dimensionless radial velocity, UD/α

v : Dimensionless angular velocity, VD/α

Greek Symbols

α : Thermal diffusivity

β : Thermal expansion coefficient

θ : Angular coordinate

ϕ : Dimensionless fluid temperature, $(T-T_0)/(T_0-T_\infty)$

ϕ_f : Dimensionless fin temperature, $(T_0-T)/(T_0-T_\infty)$

*Member, Dong-A University.

ν : Kinematic viscosity
ρ : Density
Ψ : Stream function
ψ : Dimensionless stream function, Ψ/α
w : Vorticity

Subscripts

f : Fin
f_d : Downward projecting fin
f_u : Upward projecting fin
o : Cylinder surface
S : Smallest
T : Total

Superscripts

$-$: Mean value
m : Current iteration number

1. Introduction

Many theoretical and experimental studies have been performed on natural convection from simple surfaces such as vertical plates and horizontal circular cylinders. It is of interest in natural convection heat transfer to study how the buoyancy-induced flow from one heated source affects another object which is in contact with or separated from the source. Numerical solutions for wall and free plumes above a heated vertical Plate have been carried out for $Pr=0.7-10$ by Sparrow et al.[1].

Free plume is created by the buoyancy flow above a heated plate and a typical wall plume is the flow along vertical adiabatic extension above the heated plate. Numerical solutions for two vertical plates situated one above the other have been obtained to determine the enhancement of heat transfer on the upper plate as the vertical separation distance, lateral offset and plate length are changed by Sparrow and Patankar[2] and Sparrow and Samie[3].

Buoyancy-induced flow due to multiple isolated heated elements located on a vertical surface has been studied analytically for obtaining the general nature of the flow and the dependence of the heat transfer from an element, located in the wake of another at a Prandtl number of 0.7 by Jaluria[4] An analytical study of conjugate natural convection heat transfer from an infinitely long vertical plate fin has recently carried out by Kwon and Kuehn[5].

In the present work, natural convections from two long axial fins projecting vertically from an isothermal horizontal circular cylinder are studied as fin conduction, Prandtl number and Rayleigh number are varied parametrically.

2. Numerical Analysis

The geometry investigated is shown schematically in Fig. 1. Two long vertical fins are attached to the heated isothermal cylinder at $\theta=0°$ and $\theta=180°$. It is assumed that the temperature at the base of each fin is the same as the temperature of the cylinder to which it is attached so that contact resistance is negligible. The finned cylinder is immersed into a fluid of infinite extent.

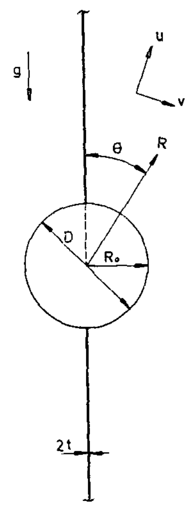

Fig. 1 Schematic diagram of the geometry investigated

The fluid flow is assumed to be steady, laminar and two-dimensional, with a plane of symmetry passing vertically through the center of the cylinder and fins. The fluid is assumed to be incompressible and to follow the Boussinesq approximation. Radiation is neglected in the computations.

The dimensionless equations for steady, laminar, natural convection flow can be written in cylindrical polar coordinates as follows:

$$\nabla^2\psi=-w \tag{1}$$

$$\nabla^2 w=\frac{1}{Pr}\left(u\frac{\partial w}{\partial r}+\frac{v}{r}\frac{\partial w}{\partial \theta}\right)-Ra\left(\sin\theta\frac{\partial\phi}{\partial r}+\frac{\cos\theta}{r}\frac{\partial\phi}{\partial\theta}\right) \tag{2}$$

$$\nabla^2\phi=u\frac{\partial\phi}{\partial r}+\frac{v}{r}\frac{\partial\phi}{\partial\theta} \tag{3}$$

$$\text{where } \nabla^2=\frac{\partial^2}{\partial r^2}+\frac{1}{r}\frac{\partial}{\partial r}+\frac{1}{r^2}\frac{\partial^2}{\partial\theta^2} \tag{4}$$

The boundary conditions become

$$u=v=\psi=0,\quad w=-\frac{\partial^2\psi}{\partial r^2},\quad \phi=1 \tag{5}$$

on the cylinder surface,

$$u=v=\psi=0,\quad w=-\frac{1}{r^2}\frac{\partial^2\psi}{\partial\theta^2},\quad C_f\frac{\partial^2\phi}{\partial r^2}=-\frac{1}{r}\frac{\partial\phi}{\partial\theta} \tag{6}$$

on the impermeable fin surface at which the thin fin approximation is used.

The outer boundary must be treated as one part with fluid coming into the solution domain, the other with fluid leaving. The fluid is assumed to approach the cylinder radially at ambient fluid temperature.

The inflow boundary conditions are

$$v=\frac{\partial^2\psi}{\partial r^2}=\phi=0,\quad w=-\frac{1}{r^2}\frac{\partial^2\psi}{\partial\theta^2} \tag{7}$$

The fluid is assumed to leave radially in the vicinity of the plume with negligible radial temperature gradient.

The outflow boundary conditions become

$$v=\frac{\partial^2\psi}{\partial r^2}=\frac{\partial\phi}{\partial r}=0,\quad w=-\frac{1}{r^2}\frac{\partial^2\psi}{\partial\theta^2} \tag{8}$$

The position of the outer boundary is fixed so that it has no significant effect on the heat transfer from either the fin or the cylinder.

In most case the outer boundary was set near $R/D\cong 6$.

The grid spacing in the angular direction is 10° although near the surfaces of fins it is reduced in steps to $\Delta\theta_s=0.625°$ to better resolve the angular gradients at the fluid-fin boundary.

The radial grid spacing varies from $\Delta r_s=0.005$ near the cylinder surface for good resolution of radial gradients to $\Delta r=1.28$ near the outer boundary of the computational domain. The resulting grid is 35×29 with a total of 1015 nodes. An indication of the magnitude of truncation errors associated with the finite differencing is given by a comparison with the results of reference (6) which are extrapolated to zero radial grid spacing for a free cylinder without fins. The difference in total heat transfer between the present results with no fin and those of (6) is 0.44% for $Ra=10^6$ and $Pr=5$.

The solutions were considered to be converged when the stream function and temperature both met the following criterion.

$$\left|\frac{B^n-B^{n-1}}{B^n}\right|<10^{-3} \tag{9}$$

where B is either ψ or ϕ, Calculations were performed on a DEC PDP 11/34 minicomputer with a Fortran program. Average solution times were approximately 3 hours.

The following definitions are used when evaluating the heat transfer. Local Nusselt number on the cylinder:

$$Nu_0=\frac{hD}{k}=-\frac{\partial\phi}{\partial r}\bigg|_{r=0.5}=\frac{q_0 D}{k\Delta T} \tag{10}$$

Local Nusselt number on the fins:

$$Nu_f=\frac{h_f D}{k}=\left|\frac{1}{\phi_f}\frac{\partial\phi}{r\partial\theta}\right|_{\theta=0\text{ or }\pi} \tag{11}$$

Cylinder total heat transfer per unit length:

$$\frac{Q_0}{\pi k\Delta T}=\frac{\bar{h}D}{k}=\overline{Nu}_0 \tag{12}$$

Fin total heat transfer per unit length of cylinder:

$$\frac{Q_f}{\pi k\Delta T}=\frac{\bar{h}_f D}{k}=\overline{Nu}_f \tag{13}$$

Total heat transfer per unit length of cylinder:

$$\frac{Q_T}{\pi k\Delta T}=\frac{Q_0+Q_f}{\pi k\Delta T}=\frac{\bar{h}_T D}{k}=\overline{Nu}_T \tag{14}$$

where $\overline{Nu}_0$, $\overline{Nu}_f$ and $\overline{Nu}_T$ denote equivalent mean Nusselt numbers based on the cylinder diameter, D.

3. Results and Discussion

Solutions were obtained for the following sets of conditions;

$0.1\leq C_f\leq 0.6$ at $Ra=10^6$, $Pr=5$,

$0.1\leq Pr\leq 10$ at $Ra=10^6$, $C_f=0.5$

and $10^3\leq Ra\leq 10^6$ at $Pr=5$, $C_f=0.5$.

Emphasis was placed on the effect of the buoyancy-induced upflow from a heated cylinder on two projecting fins and the effect of the upflow from two projecting fins on the cylinder.

Streamlines and isotherms with and without two

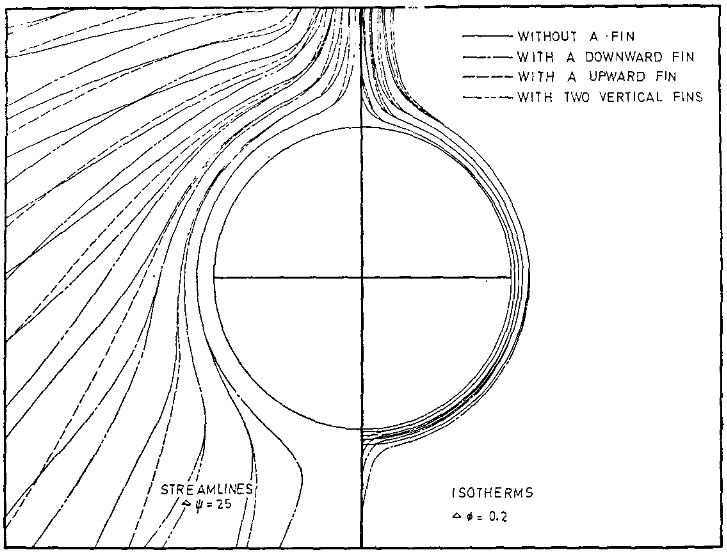

Fig. 2 Dimensionless stream lines and isotherms for a horizontal isothermal circular cylinder with two long axial fins, $Ra=10^6$, $Pr=5$, $C_f=0.5$

long vertical fins are shown in Fig. 2.

In all solutions the flow around the cylinder is more activated in the presence of the heated fins.

This is caused by the buoyancy-induced upflow from a downward projecting fins and by the buoyancy-enhanced upflow in the plume area from an upward projecting fin. However the heat transfer convected from the cylinder surface decreases below that for a bare cylinder because of the heated fluid from a downward projecting fin passing near the cylinder surface.

The mean Nusselt numbers for a horizontal isothermal circular cylinder with two long axial fins are shown in Fig. 3 as a function of the dimensionless

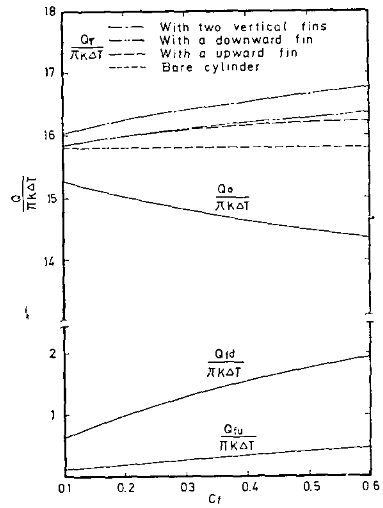

Fig. 3 Equivalent mean Nusselt numbers for a horizontal isothermal circular cylinder with two long axial fins versus C_f at $Ra=10^6$, $Pr=5$

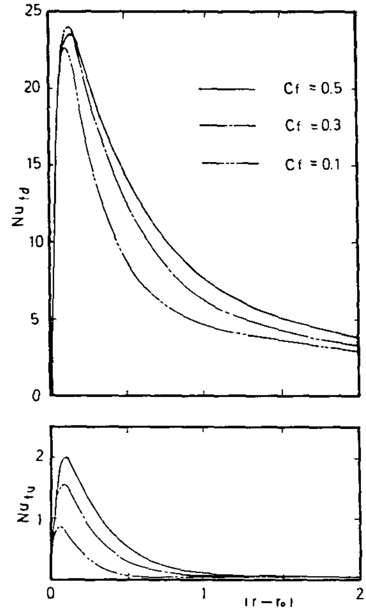

Fig. 4 Local fin Nusselt numers versus vertical position for an upward and a downward projecting fins at $Ra=10^6$, $Pr=5$

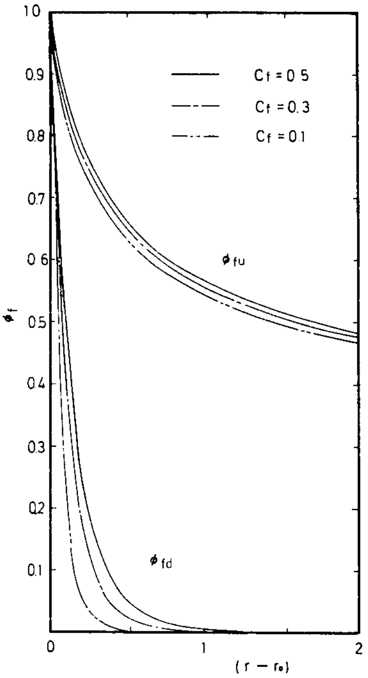

Fig. 5 Dimensionless fin temperature distributions versus vertical position for an upward and a downward projecting fins at $Ra=10^6$, $Pr=5$

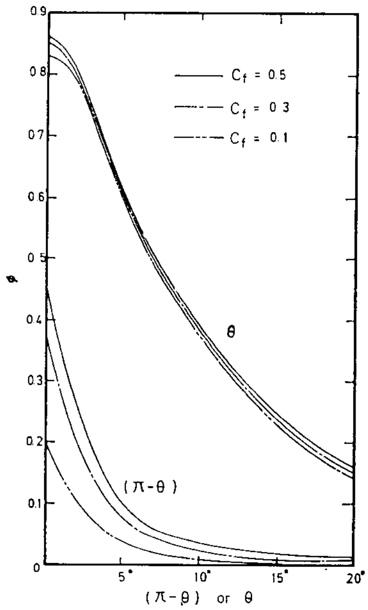

Fig. 6 Dimensionless angular temperature profiles at $(r-r_0)=0.120$ adjacent to an upward and a downward projecting fins at $Ra=10^6$, $Pr=5$

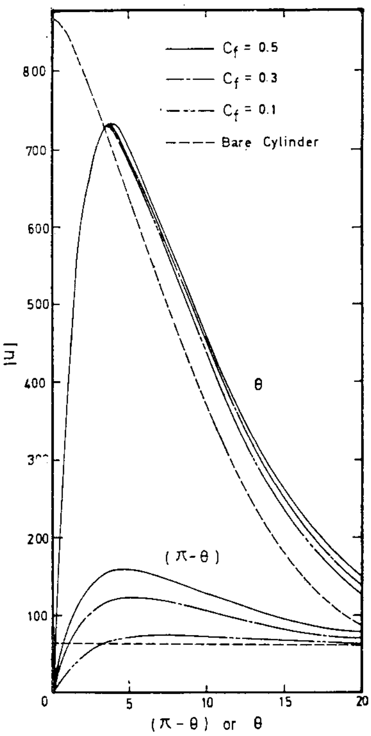

Fig. 7 Dimensionless radial velocity profiles versus angular displacement near a cylinder with an upward and a downward projecting fins at $(r-r_0)=0.192$, $Ra=10^6$, $Pr=5$

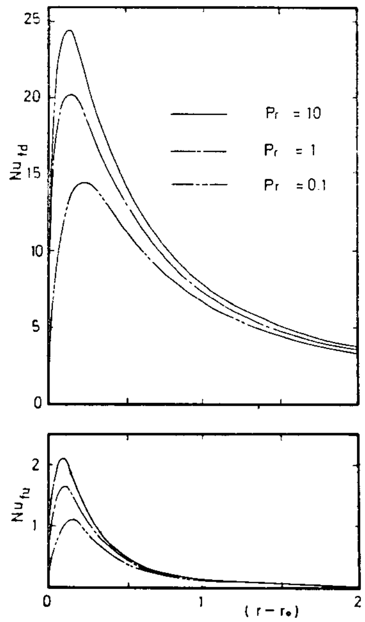

Fig. 8 Local fin Nusselt numbers versus vertical postion for an upward and a downward projecting fins at $Ra=10^6$, $C_f=0.5$

fin parameter, C_f.

The mean fin Nusselt number increases apparently as C_f is increased. This is caused by the increase in fin temperature which results in a larger total buoyant force. The mean cylinder Nusselt number decreases apparently as C_f is increased due to the decrease of the temperature gradients near the fin base. The result is an increase in the mean total Nusselt number for the cylinder with two fins as C_f is increased. Natural convection heat transfer from a horizontal circular cylinder with an upward fin, a downward fin and two fins is increased by 2.43 %, 2.86% and 5.32%, respectively, over that for a bare cylinder at $Ra=10^6$, $Pr=5$ and $C_f=0.5$.

Local fin Nusselt number distribution for various C_f is shown in Fig. 4. Generally the local fin

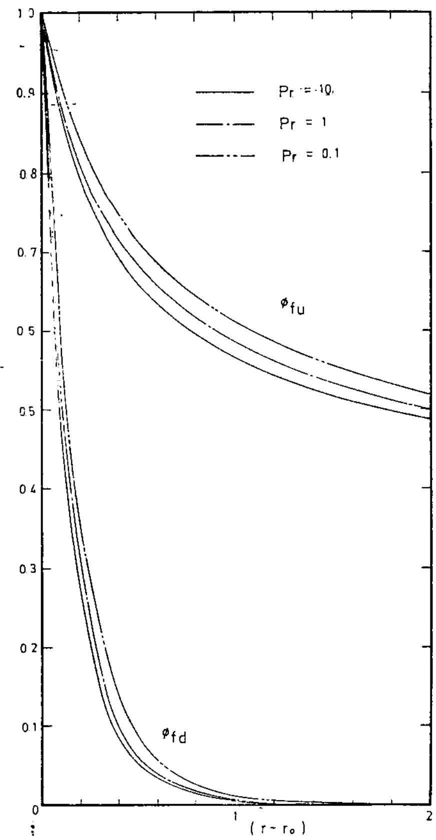

Fig. 9 Dimensionless fin temperture distributions versus vertical position for an upward and a downward projecting fins at $Ra=10^6$, $C_f=0.5$

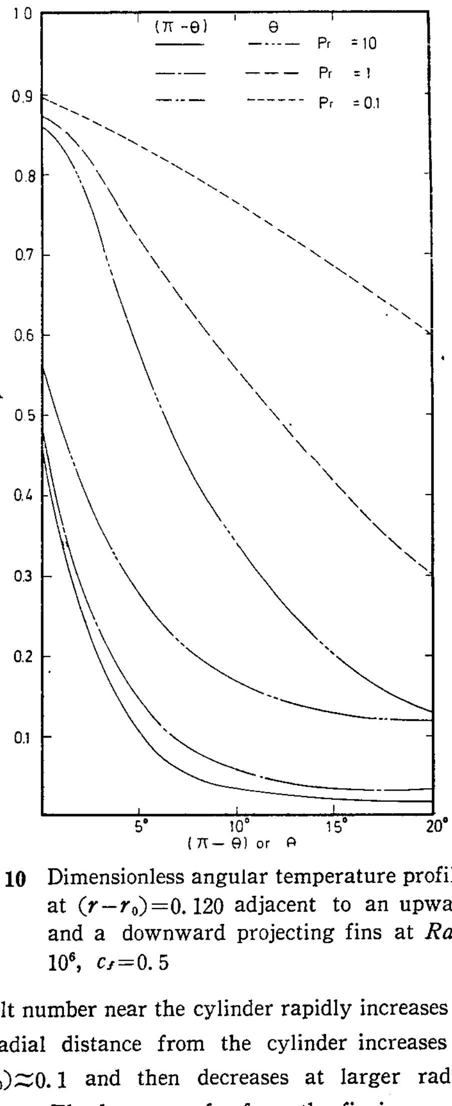

Fig. 10 Dimensionless angular temperature profiles at $(r-r_0)=0.120$ adjacent to an upward and a downward projecting fins at $Ra=10^6$, $C_f=0.5$

Nusselt number near the cylinder rapidly increases as the radial distance from the cylinder increases to $(r-r_0)\simeq 0.1$ and then decreases at larger radial distances. The heat transfer from the fin is zero at the base because of the negligible angular temperature gradient in the fluid.

The dimensionless temperature distribution on the downward fin rapidly decreases near the cylinder and then approaches the ambient temperature of the fluid at $(r-r_0)\simeq 0.7$ for $C_f=0.1$, $(r-r_0)\simeq 1.2$ for $C_f=0.3$ and $(r-r_0)\simeq 1.8$ for $C_f=0.5$ while the dimensionless temperature distribution on the upward fin gradually decreases at the radial distance from the cylinder increases as with the fluid in the plume and the effect of C_f is very small as shown in Fig.5.

The dimensionless angular temperature profiles in the fluid at $(r-r_0)=0.12$ near an upward and a downward fin are shown in Fig. 6. The temperature gradient adjacent to the fin increases as C_f increases indicating a larger local heat flux.

The dimensionless radial velocity distributions at $(r-r_0)=0.192$ above and below a cylinder with two long vertical fins for various values of C_f are shown in Fig. 7. The radial velocity is zero on the surface of the fin. The velocity is larger than the bare cylinder value near the fin because the heated fin provides additional buoyancy-induced upflow to the fluid which increases with increasing fin conductivity.

The radial velocity near the upward fin is not significantly influenced by changing C_f. Local fin Nusselt number on two projecting fins for various Prandtl numbers are shown in Fig. 8. The local fin

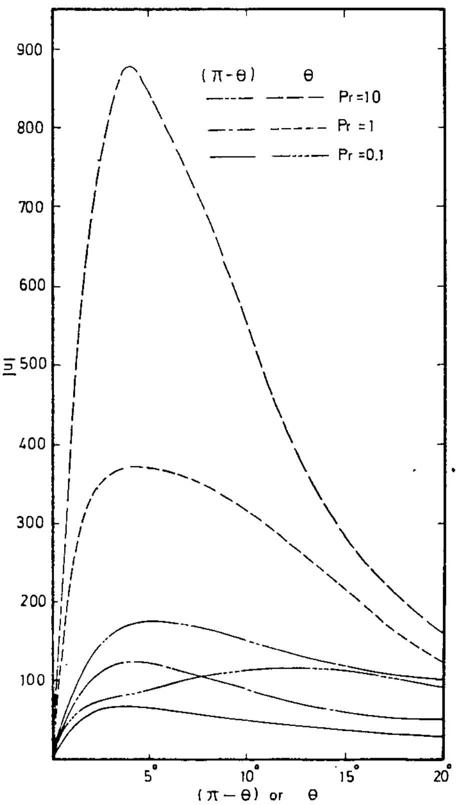

Fig. 11 Dimensionless radial velocity profiles versus angular displacement near a cylinder with an upward and a downward projecting fins at $(r-r_0)=0.192$, $Ra=10^6$, $C_f=0.5$

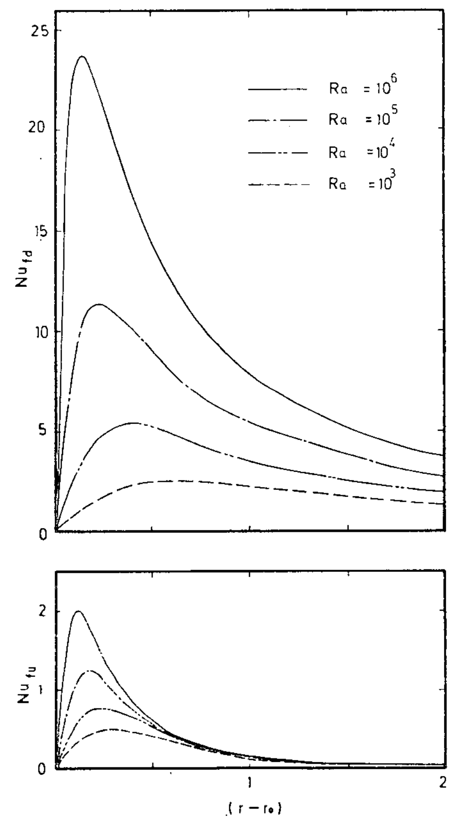

Fig. 12 Local fin Nusselt numbers on an upward and a downward projecting fins at various Rayleigh numbers for $Pr=5$, $C_f=0.5$

Nusselt number increases as Prandtl number increases in accordance with standard boundary layer theory. Dimensionless temperature distributions on two projecting fins are shown in Fig. 9.

The dimensionless fin temperature decreases as Prandtl number increases and approaches zero for the downward fin at $(r-r_0)=1.8$, 1.4 and 1.2 for $Pr=0.1$, 1 and 10 respectively. Corresponding dimensionless angular temperature distributions in the fluid at $(r-r_0)=0.120$ are shown in Fig. 10. The thermal boundary layer on the fins decreases in thickness and magnitude as Prandtl number increases.

Dimensionless radial velocity profiles in the fluid at $(r-r_0)=0.192$ are shown on Fig. 11.

The radial velocity distribution increases significantly in the fluid near the upward fin as Prandtl

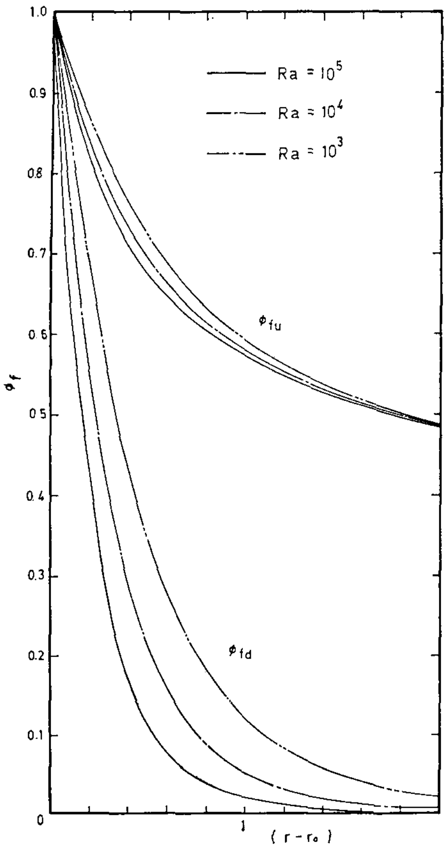

Fig. 13 Dimensionless fin temperatuse distributions on an upward and a downward projecting fins at various Rayleigh numbers for $Pr=5$, $C_f=0.5$

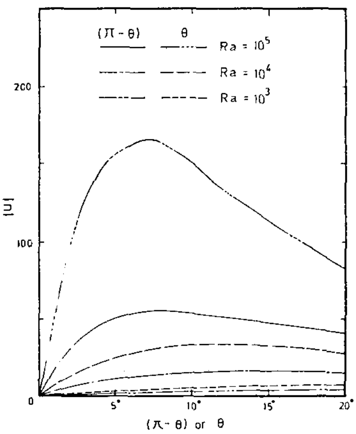

Fig. 15 Dimensionless radial velocity profiles versus angular displacment near a cylinder with an upward and a downward projecting fins at$(r-r_0)=0.192$, $Pr=5$, $C_f=0.5$

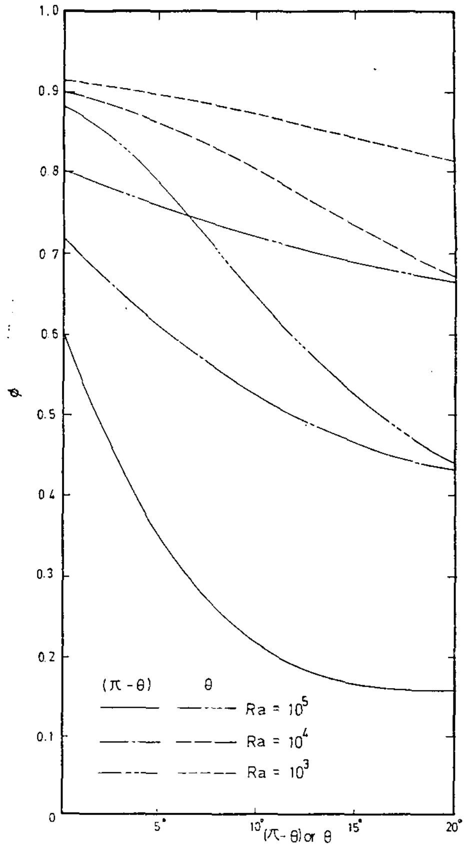

Fig. 14 Diemnsionless angular temperature profiles at $(r-r_0)=0.120$ adjacent to an upward and a downward projecting fins at $Pr=5$, $C_f=0.5$

number increases.

Local fin Nusselt number distributions on two projecting fins are shown in Fig. 12. Local fin Nusselt number distribution apparently increases as Rayleigh number increases.

Dimensionless fin temperature distribution decreases as Rayleigh number increases as shown in Fig. 13.

Dimensionless temperature profile in the fluid near the fins at $(r-r_0)=0.12$ decreases as Rayleigh number increases as shown in Fig. 14.

Dimensionless radial velocity profile at $(r-r_0)=0.192$ increases as Rayleigh number increases near the fins as shown in Fig. 15.

Finally, the flow near the plume area for a circular cylinder with two projecting fins is more activated by increasing Rayleigh number and Prandtl number

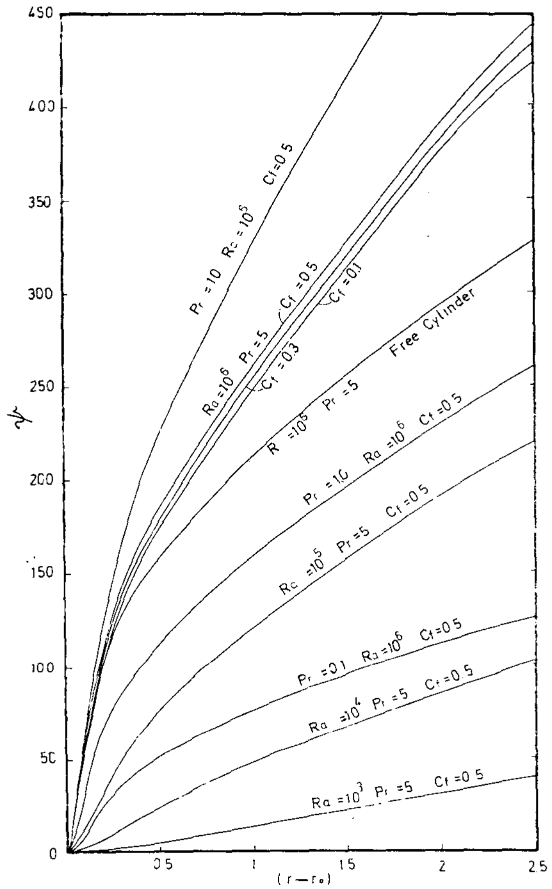

Fig. 16 Dimensionless stream function distributions at $\theta=20$ for a circular cylinder with two vertical projecting fins

but little by increasing C_f as dimensionless stream function distributions at $\theta=20°$ shown in Fig. 16.

4. Conclusions

The following conclusions can be made on the basis of the results presented above.

(1) Natural convention heat transfer around a horizontal circular cylinder with two long projecting fins is increased 5.32% over that for a bare cylinder at $Ra=10^6$ $Pr=5$ and $C_f=0.5$.

(2) Local fin Nusselt number distributions increase and dimensionless fin temperature distributions decrease as Ra and Pr increases respectively. But as C_f increases, local fin Nusselt number and dimensionless fin temperature distributions increase.

(3) Maximum local fin Nusselt number appears at $(r-r_0)=0.1-0.2$ fo the upward and downward fins projected from an isothermal circular cylinder at $Ra=10^6$

(4) The buoyancy-induced flow around a cylinder with two vertical projecting fins is stronger than that of a bare cylinder.

References

(1) E.M. Sparrow, S.V. Patankar, and R.M. Abdel-Wahed; "Development of wall and Free Plumes above a Heated Vertical Plate", ASME Journal of Heat Transfer, Vol. 100, 184~190, 1978

(2) E.M. Sparrow, and M. Faghri; "Natural Convection Heat Transfer from the upper plate of a Colinear, Separated Pair of Vertical Plates", ASME Journal of Heat Transfer, Vol. 102, 623~629, 1980

(3) E.M. Sparrow, and F. Samie; "Natural Convection Analysis of Two Laterally Misaligned Vertical Plates Situated One above the Other", Numerical Heat Transfer, Vol. 4, 427~446, 1981

(4) Y. Jaluria, "Buoyancy-Induced Flow due to Isolated Thermal Sources on a Vertical Surface," Mechanical Engineering Department, Rutgers University, 1980.

(5) S.S. Kwon, and T.H. Kuehn; "Conjugate Natural Convection Heat Transfer from a Horizontal Cylinder with a Long vertical Longitudinal Fin", Numerical Heat Transfer, Vol. 6, 84~102, 1983

(6) T.H. Kuehn, and J.L. Balvanz; "Conjugate Heat Transfer by Natural Convection from a Horizontal Heat Exchanger Tube", Proc. 7th Int. Heat. Transfer Conference, Vol. 2, 317~322, 1982

(7) T.H. Kuehn and R.J. Goldstein; "Numerical Solution to the Navierstokes Equations for Laminar Convection about a Horizontal Isothermal-Circular Cylinder", Int. J. Heat Mass Transfer, Vol. 23, 971~979, 1980